0026-895X/04/6504-842–850$20.00
MOLECULAR PHARMACOLOGY
Vol. 65, No. 4
2874/1136433
Mol Pharmacol 65:842–850, 2004
Printed in U.S.A.

Differential Roles of Arg97, Asp293, and Arg108 in Enzyme Stability and Substrate Specificity of CYP2C9

Leslie J. Dickmann, Charles W. Locuson, Jeffrey P. Jones, and Allan E. Rettie

Department of Medicinal Chemistry, University of Washington, Seattle, Washington

Received August 4, 2003; accepted December 12, 2003

This article is available online at http://molpharm.aspetjournals.org

ABSTRACT

CYP2C9 metabolizes a wide range of drugs, many of which are negatively charged at physiological pH. Therefore, it has been thought that complementarily charged amino acid(s) are critically involved in substrate binding. Previous studies have implicated arginine residues at positions 97, 105, and 108 and aspartate at position 293 in the normal catalytic function of the enzyme. To elucidate the role of these amino acids in the substrate specificity of CYP2C9, a series of mutants were constructed and analyzed for functional activity, thermal stability, and ligand binding. Charge-modifying mutations at positions 97, 105, and 293 decreased catalytic activity toward diclofenac, (*S*)-warfarin, and pyrene in a substrate-independent manner with Arg105 the least, and Arg97 the most, sensitive amino acids in this regard. Decreases in functional activity paralleled thermal instability of the mutants, suggesting that loss of function reflects more generalized structural changes rather than the absence of a specifically charged amino acid at these three positions. The R108H mutant was inactive toward all three substrates because of unexpected nitrogen ligation to the heme. Conversely, the R108F mutant exhibited substrate-dependent catalytic behavior, with almost complete loss of activity toward (*S*)-warfarin and diclofenac, but preservation of pyrene metabolism. In addition, the R108F mutation abrogated the Type I difference spectra induced by flurbiprofen and benzbromarone, obligate anions at physiological pH. These data identify critical roles for Arg97 and Asp293 in the structural stability of the enzyme and demonstrate a selective role for Arg108 in the binding and metabolism of negatively charged substrates of CYP2C9.

CYP2C9 is the major CYP2C isoform found in the human liver, constituting from 18 to 30% of total hepatic P450 (Lasker et al., 1998; Rodrigues and Lin, 2001). CYP2C9 exhibits a preference for substrates that are weak acids and participates in the oxidation of the endogenous eicosanoid, arachidonic acid, to several isomeric epoxides (Daikh et al., 1994), some of which seem to play an important role in the regulation of vascular homeostasis (Fisslthaler et al., 2000; Busse et al., 2002). Another prominent function of CYP2C9 is the oxidative metabolism of many clinically important drugs such as (*S*)-warfarin, phenytoin, and many of the nonsteroidal anti-inflammatories (Miners and Birkett, 1998). Because CYP2C9 is one of the most important human P450s involved in xenobiotic metabolism there is considerable interest in determining the precise mechanisms whereby substrates are targeted, bound in the active site, and oriented for regioselective and stereoselective oxidation.

Because CYP2C9 exhibits selectivity for substrates and inhibitors that are lipophilic and either weakly acid or neutral, it would be expected that important ligand interactions would occur with hydrophobic and hydrogen bond donor or acceptor residues in the active site of the enzyme. Previous site-directed mutagenesis studies have provided evidence in support of a role for Phe114, Val113, and Phe476 in hydrophobic interactions with (*S*)-warfarin and diclofenac and with the inhibitor sulfaphenazole (Haining et al., 1999; Melet et al., 2003). Using a variety of computer modeling techniques several groups, including our own, have proposed Arg97, Arg105, Arg108, and/or Asp293 as important charged residues in CYP2C9 (Payne et al., 1999; Rao et al., 2000; De Groot et al., 2002). In addition, alanine scanning mutagenesis of B-C loop residues 97 to 108 in CYP2C9 has provided experimental evidence that Arg97 and Arg108 are determinants of catalytic function (Ridderstrom et al., 2000), although it is not clear whether these two amino acids contribute to the general structural stability of the enzyme or contribute via polar interactions with CYP2C9 substrates.

To obtain a more detailed picture of the role that prominent charged residues play in CYP2C9 catalysis, we replaced the Arg at positions 97, 105, and 108 with Phe and His to progressively eliminate the positive charge and neutralized the I-helix acid Asp293. Mutants were purified and charac-

This research was supported in part by United States Public Health Service Grant GM32165. L.J.D. was also supported by the Hope Barnes Fellowship.

This work was presented at the European ISSX Meeting in Dijon, France in April 2003.

ABBREVIATIONS: P450, cytochrome P450; HPLC, high-performance liquid chromatography.

terized by spectroscopic and thermal stability analyses and with regard to their catalytic activity toward model substrates. The results suggest that whereas Arg97 and Asp293 are necessary for maintaining the structural integrity of the enzyme, Arg108 is a key determinant of binding and metabolism of negatively charged substrates by CYP2C9. The latter finding would not be predicted from the newly available crystal structure of CYP2C9 (Williams et al., 2003), and reasons for this apparent discrepancy are discussed.

Materials and Methods

Chemicals and Reagents

Oligonucleotides were purchased from Invitrogen (Carlsbad, CA), hydroxyapatite was purchased from Bio-Rad (Hercules, CA), and restriction enzymes were purchased from New England BioLabs (Beverly, MA). Octyl-Sepharose, flurbiprofen, diclofenac, 7-ethoxycoumarin, dNTPs, δ-aminolevulinic acid, dithiothreitol, sodium dithionite, and β-NADPH were obtained from Sigma-Aldrich (St. Louis, MO). (*S*)-Warfarin was obtained by fractional crystallization and 7-hydroxywarfarin was synthesized as described previously (Bush et al., 1983). 3′-Hydroxy,4′-hydroxy, and 5′-hydroxydiclofenac were provided by Novartis (Basel, Switzerland). Pyrene and 1-hydroxy-pyrene were purchased from Supelco (Bellefonte, PA) and Acros Organics (Santa Clara, CA), respectively. Benzbromarone was synthesized as described previously (Locuson et al., 2003). Dilauryl phosphatidylcholine was purchased from Avanti Polar Lipids, Inc. (Alabaster, AL). HPLC grade solvents were purchased from Fisher Scientific Co. (Fair Lawn, NJ).

Mutagenesis and Protein Expression

The *CYP2C9* gene was subcloned into the pUC vector as described previously (Haining et al., 1999). Mutagenesis was performed using either overlap extension polymerase chain reaction (R105H, R108F, R108H, D293N, and D293V) or the Transformer site-directed mutagenesis kit (R97F, R97H and R105F; BD Biosciences Clontech, Palo Alto, CA). Mutagenic oligonucleotides consisted of the following sequences: R97F, 5′-GAG GAG TTT TCT GAA TTT GGC ATT TTC CCA CTG-3′; R97H, 5′-GAG GAG TTT TCT GGA CAT GGC ATT TTC CCA CTG-3′; R105F, 5′-TTC CCA CTG GCT GAA TTT GCT AAC AGA GGA TTT G-3′; R105H (forward), 5′-CCC ACT GGC TGA ACA TGC TAA CAG AGG ATT TG-3′; R105H (reverse), 5′-CAA ATC CTC TGT TAG CAT GTT CAG CCA GTG GG-3′; R108F (forward), 5′-GAA AGA GCT AAC (TTT) GGA TTT GGA ATT G-3′; R108F (reverse), 5′-CAA TTC CAA ATC C(AA A)GT TAG CTC TTT C-3′; D293N (forward), 5′-AAC ACT GCA GTT (AAC) TTG TTT GGA GCT-3′; D293N (reverse), 5′-AGC TCC AAA CAA (GTT) AAC TGC AGT GTT-3′. Oligonucleotides for the R108H mutant were the same as those for R108F except that the sequence in parentheses was changed to CAT in the forward primer and ATG in the reverse primer. Oligonucleotides for the D293V mutations were the same as those for the D293N mutation except that the sequence in parentheses was changed to GTC in the forward primer and GAC in the reverse primer. External primers used in amplification were: forward, 5′-ACG GCC AGT GAA TTC AAT GGA TTC TCT TG-3′; reverse; 5′-GTA CCG AGC TCG AAT TCG TCA GAT GAC-3′. The target mutation and integrity of the gene outside this locus were confirmed by DNA sequencing. CYP2C9 mutants were then subcloned into the EcoRI site of the pFastBac vector (Invitrogen). Baculovirus construction and protein expression in *Spodoptera frugiperda* cells were performed according to the Bac-to-Bac Baculovirus Expression System protocol from Invitrogen.

Protein Purification

Purification of wild-type CYP2C9 and the R108F, R108H, D293N, and D293V mutants were carried out as described previously (Haining et al., 1999) on Octyl-Sepharose and hydroxyapatite with omission of the DEAE-Sepharose step. The R97F, R97H, R105F, and R105H mutants did not bind to hydroxyapatite under standard conditions. Therefore, P450 fractions that eluted from Octyl-Sepharose were first dialyzed overnight against 2 × 1 liters of 5 mM KPi buffer, pH 7.0, 20% glycerol, and 0.1% Emulgen 911 before application to hydroxyapatite. Loosely bound enzyme was washed with 5 mM KPi, pH 7.0, 25% glycerol, and 0.2% cholate until $A_{280} < 0.02$. Emulgen-free protein was eluted with 300 mM KPi, pH 7.4, 20% glycerol, and 0.5% cholate, and all preparations were dialyzed against 2 × 1 liters of 100 mM KPi, pH 7.4, 20% glycerol, and 1 mM EDTA before storage at −80°C. Protein was measured by the Lowry method and heme concentrations were determined by the pyridine hemochromogen method using an extinction coefficient of 20.7 mM^{-1} cm^{-1} (Falk, 1964).

Liquid Chromatography/Mass Spectrometry Analysis

Intact protein molecular masses for each of the CYP2C9 mutants (monoisotopic MH^+) were obtained after chromatography on a PO-ROS2 column using a Micromass Quattro II tandem quadrupole mass spectrometer. This instrument used MassLynx software (Beverly, MA) and was run in electrospray ionization mode at a cone voltage of 30 V, source block temperature of 150°C, and a desolvation temperature of 350°C (Henne et al., 2001).

P450 Measurements

Spectral studies were performed using an Agilent 8453E UV-visible spectroscopy system unless otherwise noted. Spectral P450 contents were determined according to published methods (Estabrook and Werringloer, 1978), with the modification that methyl viologen was added in addition to dithionite at a final concentration of 1.2 μM. A difference spectrum for the R108H mutant versus wild-type CYP2C9 was obtained by adding equimolar amounts of enzyme (1 μM based on the pyridine hemochromogen values) to matched sample and reference cuvettes, respectively, and then scanning from 350 to 500 nm.

Analysis of Thermal Stability of CYP2C9 Mutants

These studies were carried out according to a modification of the protocol described by Chen et al. (1997). Each P450 preparation (5 μM) was preincubated at 48°C in 100 mM potassium phosphate buffer, pH 7.4, for 0 to 30 min. At various time points, aliquots were removed and the reduced CO difference spectra were recorded relative to the zero time point value. Half-lives for the thermally induced conversion of P450 to P420 were determined according to first-order decay kinetics.

Spectral Binding

Purified CYP2C9 was first reconstituted with extruded liposomes of dilauryl phosphatidylcholine. The final amount of lipid used was 0.2 μg/pmol of enzyme. Wild-type CYP2C9 or the R108F mutant (300 pmol) were then placed into separate cuvettes containing 50 mM potassium phosphate at pH 7.4 to a final volume of 0.5 ml. After allowing the sample and reference cuvettes to reach room temperature, difference spectra were obtained over the range 350 to 500 nm, after addition of 0 to 150 μM racemic flurbiprofen or 0 to 100 nM benzbromarone, using a double beam spectrophotometer (DW2000; Aminco, Lake Forest, CA).

General Enzyme Assay Conditions

Incubation mixtures contained 50 mM potassium phosphate, pH 7.4, 10 to 50 pmol of CYP2C9, 20 to 100 pmol of P450 reductase, 10 to 50 pmol of cytochrome b_5 (P450/reductase/cytochrome b_5, 1:2:1), 0.5 μg of dilauryl phosphatidylcholine extruded through a 0.2-μm filter (Avanti Polar Lipids), 20 μM dithiothreitol, 0.5 mM NADPH, and appropriate substrate in a final volume of 0.5 ml. All enzymatic reactions were initiated by the addition of NADPH and conducted at

37°C. Analysis of (*S*)-warfarin, diclofenac, and pyrene metabolites was performed using a Hewlett-Packard model 1050 in line with a Hewlett-Packard series 1046A fluorescence detector (Hewlett-Packard, Palo Alto, CA).

Metabolic Assays

Diclofenac. Rates of formation of 4′-hydroxydiclofenac by reconstituted enzyme mixtures were determined by HPLC as described previously (Haining et al., 1999), except that metabolic reactions were terminated after 15 min. Diclofenac concentrations ranging from 1.5 to 100 μM were used for determination of kinetic parameters.

(*S*)-Warfarin. (*S*)-Warfarin 7-hydroxylation was measured by an HPLC-fluorescence method (Lang and Bocker, 1995). The substrate concentration range used for kinetic determinations was from 2 to 100 μM.

Pyrene. Formation of 1-hydroxypyrene was determined by HPLC using a fluorometric assay with a Nucleosil C_{18} column (Agilent, Palo Alto, CA), 4.0 × 125 mm. The flow rate used was 0.8 ml/min, the column temperature was set to 40°C, and the solvents used were water (A) and methanol (B). The column was initially equilibrated with 54:46 A/B, and a linear gradient was applied from 0 to 35 min to 5:95 A/B and from 35 to 40 min back to 54:46 A/B. The column was allowed to equilibrate at 54:46 A/B for 5 min between each run. Metabolic reactions were allowed to proceed for 15 min and were then quenched with 0.1 ml of acetonitrile. Metabolite was detected fluorometrically, with excitation and emission wavelengths set at 340 nm and 390 nm, respectively, and a cut-off filter at 345 nm. For kinetic analysis, the concentrations of pyrene varied from 0.5 to 50 μM.

Kinetic Analysis

K_m and V_{max} were estimated using the k.cat program (Biometallics, Inc., Princeton, NJ) and nonlinear regression was performed using the SYSTAT program (Systat Systems, Inc., Richmond, CA).

Results

Expression, Purification, Heme Contents, and Accurate Mass of CYP2C9 Mutants. CYP2C9 mutants at amino acid positions 105, 108, and 293 all expressed well in insect cells, reaching levels that ranged from 200 to 800 nM as determined by reduced CO difference spectra (Table 1). In contrast, mutants at position 97, especially R97F, expressed at consistently low levels (≤50 nM). Mutations at positions 97 and 105 also resulted in CYP2C9 proteins that exhibited altered chromatographic properties during purification. However, modified isolation protocols were devised that permitted isolation of all mutant enzymes, although the low final yields of R97F limited some of its biochemical characterization (see below). Table 1 also shows the specific heme contents and accurate masses of intact, wild-type CYP2C9 and the mutant preparations. Mass data obtained by liquid chromatography/electrospray ionization-mass spectroscopy of the apo-enzymes agree with calculated molecular weights within an error of ≤0.01%. Specific contents ranged from 5.3 to 18.1 nmol/mg. Because SDS-polyacrylamide gel electrophoresis analysis (not shown) indicated similar high levels of purity (80–90% homogeneity), it seems that mutations at positions 97 and 293 compromise heme binding or retention in the holo-enzyme.

TABLE 1
Specific heme content and accurate mass analysis of CYP2C9 mutants

Enzyme	Expression Level	Sp. Content	Molecular Mass		Δ
			Expected	Observed	
	nmol/l	*nmol/mg*	*Da*		*Da*
CYP2C9	500	18.1	55,627	55,630	+3
R97F	≤50	5.3	55,618	–[a]	–
R97H	≤100	8.8	55,608	55,610	+2
R105F	500	14.2	55,618	55,624	+6
R105H	500	14.3	55,608	55,612	+4
R108F	500	17.4	55,618	55,619	+1
R108H	800	15.7	55,608	55,610	+2
D293N	250	8.6	55,626	55,629	+3
D293V	200	8.1	55,611	55,616	+5

[a] Analysis not performed due to insufficient amounts of the protein.

Functional Activity of CYP2C9 Mutants. The functional capabilities of the CYP2C9 mutants were investigated using the substrates diclofenac, (*S*)-warfarin, and pyrene. Both diclofenac and (*S*)-warfarin are weak acids and are considered archetypal CYP2C9 substrates. Pyrene, on the other hand, is a planar aromatic compound with no functional groups. Metabolic reactions were performed at single substrate concentrations (50 μM) that were well in excess of the wild-type K_m for each substrate. All mutants displayed compromised metabolism of at least two of the three substrates. Figure 1 illustrates the relative percentage activity remaining for each mutant, with reaction velocities for wild-type enzyme set to 100%. Phe and His mutations introduced at position 97 caused the most dramatic decreases in hydroxylation rates (>98%) for all three substrates. In contrast, Phe and His mutations at position 105 elicited much more modest effects, with the R105H mutant exhibiting 40 to 70% of wild-type activity. Substantial (>80%) and largely substrate-independent decreases in catalytic activity were also evident for the R108H mutant. However, the most striking finding was the substrate-dependent metabolic behavior of the R108F mutant, which exhibited almost complete loss of activity toward (*S*)-warfarin and diclofenac but retained a substantial proportion of the wild-type activity toward pyrene.

Steady-State Kinetics for Pyrene, Diclofenac, and (*S*)-Warfarin Catalyzed by CYP2C9 Wild-Type and the R108F Mutant. To confirm the unusual catalytic trends observed for the R108F mutant in the metabolic screen, we measured steady-state kinetics for substrate metabolism cat-

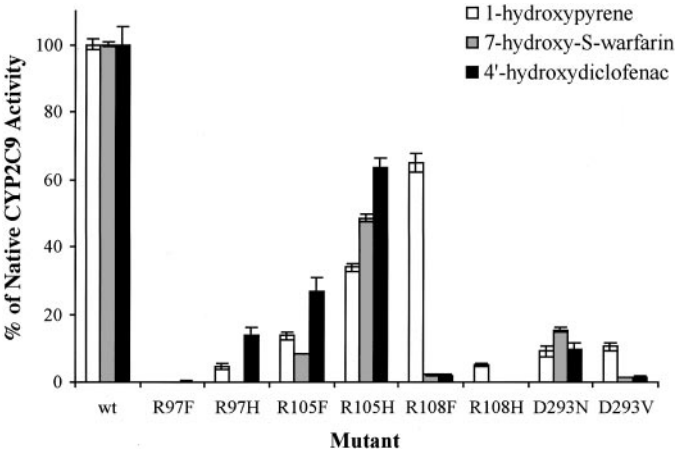

Fig. 1. Catalytic properties of CYP2C9 mutants. Diclofenac, (*S*)-warfarin, and pyrene metabolite assays were performed as described under *Materials and Methods* using 50 μM substrate. The error bars represent the S.D. from triplicate incubations.

alyzed by this mutant and the wild-type enzyme (Table 2). Over a wide substrate concentration range, diclofenac 4′-hydroxylation and (*S*)-warfarin 7-hydroxylation followed Michaelis-Menten kinetics for the wild-type enzyme, but turnover was barely detectable with the R108F mutant. In contrast, pyrene exhibited sigmoidal kinetics with both enzymes and little change in either K_{cat} or K_s. These data confirm the unique metabolic processing of pyrene by the R108F mutant.

Spectral Binding Studies. We next attempted to measure dissociation constants for substrate binding to CYP2C9 and the R108F mutant, but neither (*S*)-warfarin, pyrene, nor diclofenac, the three substrates used in the initial functional studies, elicited strong spectral changes at ligand concentrations up to 100 μM. By contrast, flurbiprofen readily formed a type I binding spectrum, as did the high-affinity inhibitor benzbromarone (Fig. 2). Titration with flurbiprofen (not shown) provided a K_d value of 21 $\pm$ 1 μM. However, the magnitude of the maximum spin state change was substantially reduced with benzbromarone, thereby precluding robust measurement of K_d for this ligand. Most significantly, spectral binding of both flurbiprofen and benzbromarone was severely attenuated in the R108F mutant (Fig. 2).

Aberrant Spectral Properties of the R108H Mutant. We then turned our attention to the mechanism underlying generalized loss of activity observed with the R108H mutant. CD spectra (not shown) of wild-type CYP2C9 and the R108F and R108H mutant enzymes provided evidence of well-folded proteins with no indication of alterations in secondary structure. However, clues to the mechanism underlying the differential catalytic properties of R108H and R108F were obtained from examination of their electronic absorption spectra. Wild-type CYP2C9 and each of the eight mutants exhibited an absorption maximum at 451 nm for the Fe^{2+}-CO complex (Table 3). However, we noted that CO binding to dithionite-reduced P450 occurred extremely slowly and incompletely over the course of an hour. In addition, the ferric form of the R108H mutant exhibited an absorption maximum at 426 nm, with a similar red shift in the α and β bands and a β/α ratio of 1.3:1 (Fig. 3). These spectral properties are characteristic of a nitrogenous ligand bound form of ferric P450 (Dawson et al., 1982), in contrast to that of the typical low-spin ferric species evident for all the other mutant forms of the enzyme investigated here (Table 3). Further evidence for this assignment is provided by the inset in Fig. 3, which shows a type II difference spectrum obtained when the wild-type enzyme was referenced against an equimolar concentration of the R108H mutant. Collectively, these data suggest that the imidazole group of the R108H mutant serves as the sixth ligand to the ferric enzyme and is only very slowly displaced upon reduction, thereby resulting in a substrate-independent loss of catalytic activity.

Thermal Stability of CYP2C9 Mutants. Finally, we probed the generalized loss of function for the Arg97 and Asp293 mutants by evaluating their thermal stability. A variety of conditions, including high temperature, has been shown to convert P450 to P420, an inactive form of the enzyme (Martinis et al., 1996; Chen et al., 1997). Therefore, we determined the effect of preincubation at 48°C for 0 to 30 min on the stability of the reduced P450-CO complex for each mutant. Data are shown graphically in Fig. 4, and the calculated half-lives of the P450-to-P420 conversion are shown in Table 4. Mutations at residue 105 exhibited the most modest effects, with near equivalent half-lives of 13 to 17 min for the conversion of cytochrome P450 to P420 in the wild-type, R105F, and R105H forms of the enzyme. In contrast, mutations introduced at position 108 led to protein products that were more stable than wild-type, with the R108F and R108H mutants exhibiting half-lives of 24 and 177 min, respectively. At zero time, only the R97H mutant exhibited significant (>10%) amounts of P420. Indeed this mutant proved to be the most thermally unstable in that no spectral P450 was detectable after a 5-min incubation at 48°C. Mutations introduced at residue 293 also led to enzymes that were much less stable than wild-type, exhibiting half-lives of 2 to 3 min.

Discussion

Many CYP2C9 substrates possess at least two noncoplanar aromatic rings and anionic and/or hydrogen bond acceptor sites located 6 to 10 Å from the hydroxylation site (Ekins et al., 2001). Therefore, it is reasonable to expect that interactions with both hydrophobic and charged residues in the active site of the enzyme will dictate substrate binding to CYP2C9. Site-directed mutagenesis studies (Haining et al., 1999; Melet et al., 2003) have suggested important roles for the hydrophobic residues Phe114, Val113, and Phe476 in ligand interactions; however, the nature of polar or charge interactions that dictate the binding and metabolism of acidic substrates have not been clarified.

During preparation of this manuscript, a crystal structure of CYP2C9 with (*S*)-warfarin bound was reported (Williams et al., 2003). Whereas aromatic interactions with active-site Phe residues were again highlighted, the structure did not identify polar or charged amino acid interactions with (*S*)-warfarin. In this structure, (*S*)-warfarin occupied a distal binding pocket in a relatively capacious active site such that the position of hydroxylation on the coumarin nucleus approaches no closer than 10 Å to the heme. The authors speculated that this 'warfarin binding site' is too distant for

TABLE 2

Steady-state kinetic parameters for substrate metabolism catalyzed by CYP2C9 and the R108F mutant

The error values represent the standard deviation calculated from the best fit values of the curves derived from the Michaelis-Menten [diclofenac and (*s*)-warfarin] or Hill equations (pyrene). The Hill coefficients for CYP2C9 and the R108F were 2.2 and 1.8, respectively.

	(S)-Warfarin			Diclofenac			Pyrene	
Enzyme	K_{cat}	K_m	K_{cat}/K_m	K_{cat}	K_m	K_{cat}/K_m	K_{cat}	K_s
	min^{-1}	μ*M*	*ml/nmol P450/min*	*min*$^{-1}$	μ*M*	*ml/nmol of P450/min*	*min*$^{-1}$	μ*M*
CYP2C9	0.15 $\pm$ 0.01	5.6 $\pm$ 0.2	0.03	25.2 $\pm$ 2.0	4.5 $\pm$ 0.2	5.6	0.36 $\pm$ 0.06	3.3 $\pm$ 0.6
R108F	<0.01	—[a]	—[a]	<1	—[a]	—[a]	0.28 $\pm$ 0.05	2.9 $\pm$ 0.6

[a] Not determined due to low turnover.

effective hydroxylation and may represent an initial recognition site, or allosteric site, in the enzyme. Thus, much remains to be learned about ligand interactions with charged amino acids residues in CYP2C9, particularly as they relate to catalytically productive turnover with disparate types of substrates.

Experimental Approach

To probe the functional role of prominent charged residues in CYP2C9, we constructed sets of His and Phe mutants at positions 97, 105, and 108 to progressively eliminate the positive charge at these positions and maintain, as much as possible, the steric bulk of the substituent. In addition, we constructed mutants at position 293 in which a conserved Asp residue is found in most CYP2 isoforms. This residue has been implicated in CYP2C9's interactions with sulfaphenazole and coumarin derivatives on the basis of homology modeling (Jung et al., 1998; Rao et al., 2000), and the orthologous amino acid in CYP2C5 (D290) is a substrate contact residue in one of the conformations of the enzyme that has been crystallized with a sulfaphenazole analog (Wester et al., 2003). Therefore, Asn and Val substitutions were made specifically to neutralize the acidic charge at position 293 in CYP2C9 while again maintaining steric bulk. The study design further involved subjecting each of these mutants to metabolic studies with a series of substrates that progressively changed anionic and acidic character, from diclofenac (acidic and charged at physiological pH) to (*S*)-warfarin (acidic, uncharged for the ring-closed tautomer) to pyrene (nonionic and uncharged). Finally, we evaluated structural changes in the mutants from CD spectra and by determining the thermal stability of reduced P450-CO difference spectra. These experiments were designed in an attempt to differentiate between gross structural effects, instability of the active site environment, and disruption of specific polar interactions between ligand and enzyme in the loss of functional activity displayed by many of the mutant proteins. Figure 5 depicts the positions of the mutated residues in CYP2C9 based on the recent crystal structure of the highly engineered enzyme (Williams et al., 2003).

General Trends

CYP2C9 mutations that diminished or eliminated the charged group at Arg97, Arg105, or Asp293 decreased catalytic activity in a substrate-independent manner. Loss of hydroxylation activity was most marked for mutations at Arg97, with the R97F mutant essentially devoid of activity, and least evident for mutations at Arg105, where the R105H mutant retained some 70% of diclofenac hydroxylation activity. The magnitude of these functional changes closely paralleled alterations in the stability of the enzyme active site inferred from the half-life of conversion of P450 to P420 at 48°C, suggesting that loss of function reflects more generalized structural changes rather than the absence of a specifically charged amino acid at these three positions.

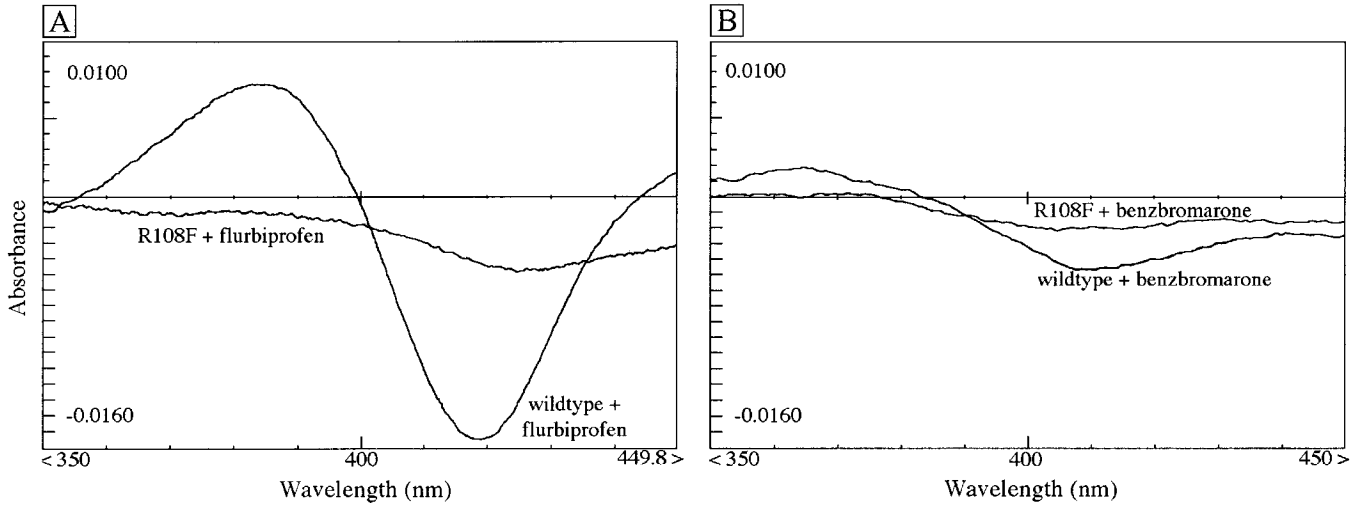

Fig. 2. Binding spectra of flurbiprofen (A) and benzbromarone (B) to wild-type CYP2C9 and the R108F mutant. Ligands (100 and 0.1 μM, respectively) were added to P450 solutions at a concentration of 0.6 μM and difference spectra were recorded as described under *Materials and Methods*.

TABLE 3

Spectral properties of CYP2C9 mutants

Spectra were recorded in 100 mM potassium phosphate buffer, pH 7.4, and contained 0.5 to 1 μM enzyme based on pyridine hemochromogen assay results

Enzyme	Fe^{2+}-CO	Fe^{3+} Soret band	Fe^{3+} α band	Fe^{3+} β band	Fe^{3+} β/α ratio
	nm	*nm*	*nm*	*nm*	
wtCYP2C9	451	418	573	534	0.96
R97F	451	418	574	535	1.02
R97H	451	419	572	535	1.01
R105F	451	418	572	535	1.03
R105H	451	418	570	536	1.01
R108F	451	418	571	536	0.98
R108H	451	426	578	545	1.27
D293N	451	417	571	534	1.04
D293V	451	418	569	534	1.11

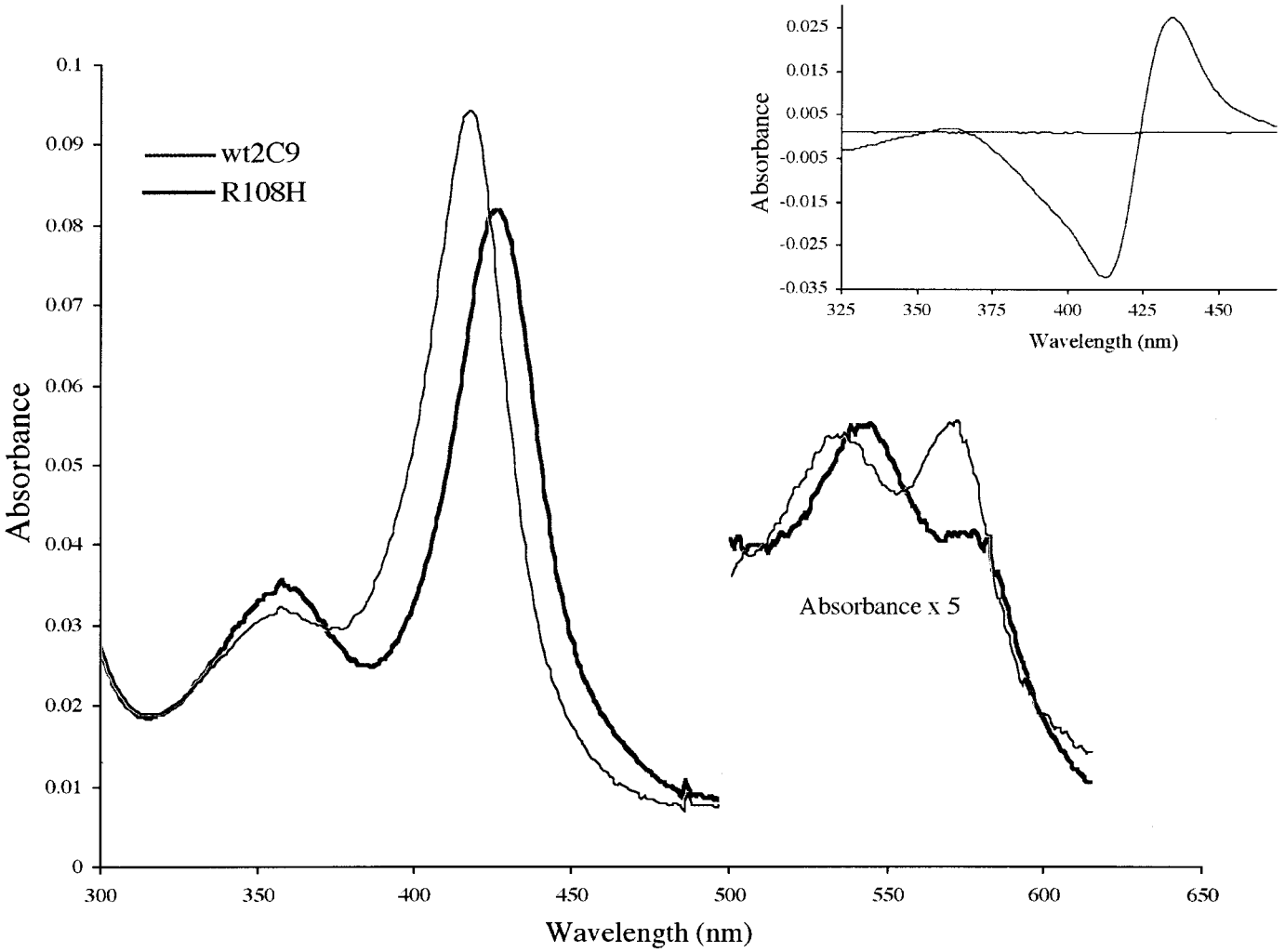

Fig. 3. Electronic Absorption Spectra of Ferric CYP2C9 and the R108H Mutant. Purified preparations of wild-type and R108H were diluted to 3 μM (based on pyridine hemochromogen assay values) and the absorption spectra recorded. Inset, type II binding spectrum observed with the CYP2C9 R108H mutant. The sample contained 1 μM protein in 100 mM potassium phosphate buffer, pH 7.4. An equimolar amount of wild-type enzyme was used as a reference. λ_{max} = 434 nm; λ_{min} = 412 nm.

Arg97. Arg97 is conserved in all members of the human CYP1, CYP2, CYP17, and CYP21 families. Notably, of all the isoforms expressed in the current study, the Arg97 mutants posed the greatest difficulties in terms of expression and stability during purification, and final preparations of the enzyme contained <50% of the expected heme content. These observations, coupled with these mutants' extreme thermal instability suggest a critical role for Arg97 in heme binding and maintenance of the structural stability of CYP2C9. [Davies et al. (2004) have also suggested a critical role for Arg97 in the protein stability of CYP2C9.] These data and conclusions complement the new structural data for CYP2C9 (Williams et al., 2003), which shows the Arg97 side chain binding between the heme propionates (see Fig. 5).

Asp293. Asp293 is an acidic I-helix residue that is highly conserved among CYP2 enzymes. It maps to Asp301 in CYP2D6, which has attracted considerable attention as a candidate for the amino acid that binds the charged amino group of many CYP2D6 substrates. Based on crystal structure information for CYP2C5, it has been suggested that Asp301 in CYP2D6 may hydrogen bond to backbone B′-C loop residues (Kirton et al., 2002). Wolf and coworkers have recently extended this interpretation to Asp293 of CYP2C9 based on site-directed mutagenesis studies in bacteria that failed to correctly incorporate heme into the D293Q and D293N mutants (Flanagan et al., 2003; Paine et al., 2003). In the present study, we found that both the D293N and D293V mutants incorporated heme to ~50% of the nominal content when expressed in insect cells, thereby permitting a fuller characterization of their effects on structure and function. Despite their relative ease of expression using the baculovirus system, the D293N and D293V mutants exhibited large decreases in catalytic function and substantial reductions in thermal stability of the P450 complex relative to native CYP2C9. In the new crystal structure of CYP2C9, Asp293 is hydrogen bonded to the backbone nitrogen of I112 (Williams et al., 2003). When coupled with the present experimental data, it would seem that that this interaction is critical to the stability of the heme environment of CYP2C9.

Arg108. The most intriguing results were those obtained with the Arg108 mutants of CYP2C9. Replacement of the positively charged Arg residue at 108 with a similarly sized, but uncharged, Phe residue caused almost complete loss of activity toward the acidic substrates diclofenac and (*S*)-war-

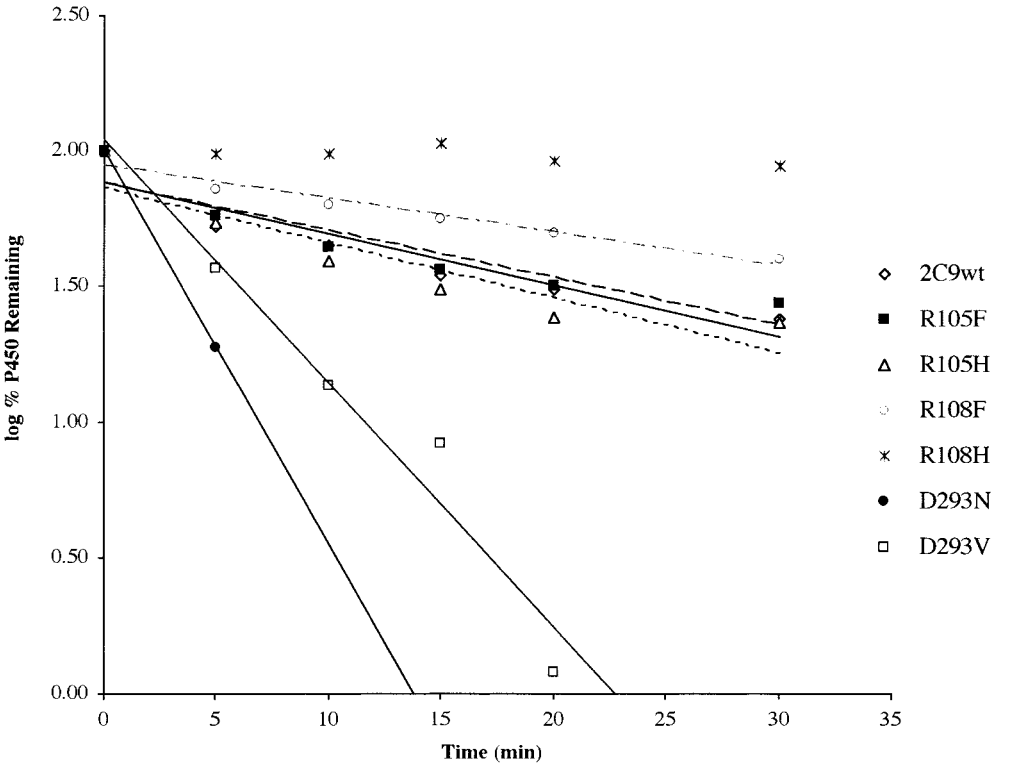

Fig. 4. Thermal stability of CYP2C9 mutants. Purified proteins were preincubated at 48°C in 100 mM potassium phosphate buffer, pH 7.4, for the indicated times, and the reduced P450-CO difference spectra were recorded. The amount of spectral P450 remaining at the indicated time point is shown relative to the zero time point. Values are the mean of duplicate determinations.

farin, but preserved the mutant's catalytic efficiency toward the unfunctionalized molecule, pyrene. Interestingly, both wild-type CYP2C9 and the R108F mutant exhibited sigmoidal kinetics for pyrene hydroxylation with Hill coefficients of 2.2 and 1.8, respectively. These atypical kinetics may reflect the proclivity of pyrene to π-stack in the active site of P450s (Dabrowski et al., 2002), but this was not investigated further at this time. The relative behavior of the R108F mutant toward pyrene is akin to that described recently for the interaction between spirosulfonamide and Glu216 mutants of CYP2D6 (Guengerich et al., 2002). In both instances, a case can be made that substitution of these key charged residues is a critical determinant of binding of their 'preferred' complementary charged substrates. To explore this, we attempted to obtain binding spectra for the substrates used for the functional analysis. However, type I spectra were difficult to obtain with either (*S*)-warfarin, diclofenac or pyrene. Conversely, flurbiprofen and benzbromarone exhibited readily observable type I binding that was abolished when the R108F mutant was used as the enzyme source. The pK_a values for flurbiprofen and benzbromarone are 4.2 and 4.5, respectively (Anderson and Conradi, 1985; Locuson et al., 2003), so both are obligate anions at physiological pH. These data provide strong evidence that Arg108 is a critical determinant of the binding of negatively charged substrates to CYP2C9.

The recent crystal structure of CYP2C9 depicts Arg108

TABLE 4
Thermal stability of CYP2C9 mutants

Enzyme	% P420 (at 0 min)	Half-Life
		min
wt2C9	0	16
R97F	—[a]	—[a]
R97H	30	<2[b]
R105F	0	17
R105H	0	13
R108F	0	24
R108H	9	177
D293N	0	2
D293V	0	3

[a] Analysis was not performed due to insufficient amounts of protein.
[b] No remaining P450 peak was observed after a 5-min preincubation at 48°C.

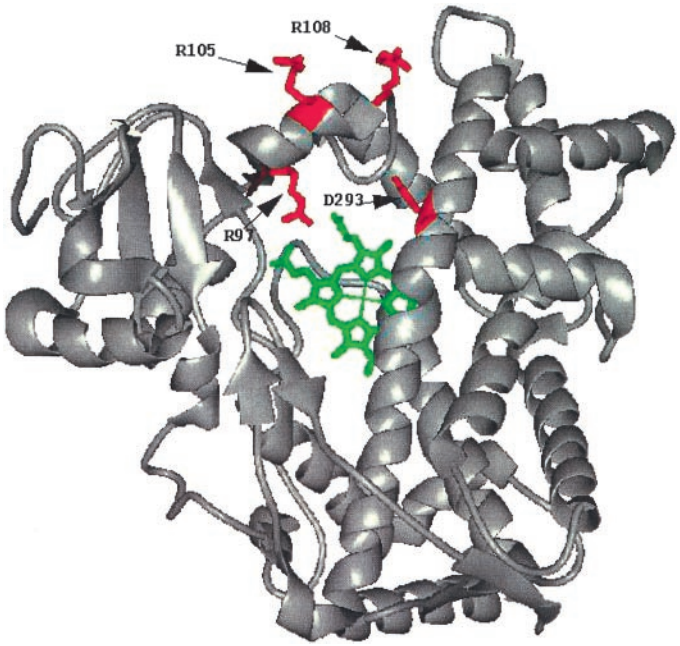

Fig. 5. Location of amino acids Arg97, Arg105, Arg108, and Asp293 in the crystal structure of engineered CYP2C9. This figure was constructed from the PDB file, 1OG5. The mutated amino acids are shown in red, and the heme is in green. Portions of the F-helix, F-G loop, and G-helix have been removed to expose the mutated residues.

pointing away from the active site, uninvolved in (*S*)-warfarin binding (see Fig. 5). Yet in the current studies, the R108F mutant abrogated (*S*)-warfarin 7-hydroxylation. To reconcile these observations, we can consider the possibility that Arg108 is critical to the initial recognition/docking of acidic ligands. Alternatively, or even additionally, it is possible that Arg108 binds (*S*)-warfarin in a more catalytically productive orientation than is evident from the recent crystal structure (Williams et al., 2003). In support of the latter scenario, crystallographic data from Dr. Eric Johnson's group show Arg108 binding to the carboxylate of flurbiprofen in the active site of CYP2C9 (Johnson et al., 2003). These emerging structural observations are very compatible with the spectroscopic and functional data presented here, that demonstrate a critical role for Arg108 in the binding of flurbiprofen and benzbromarone and in the metabolism of diclofenac and (*S*)-warfarin by CYP2C9.

Recent structural studies increasingly demonstrate that the active site of the CYP2C enzymes is quite flexible and able to bind ligands in multiple conformations (Wester et al., 2003). In this context of conformational flexibility, it is notable that the R108H mutant produced the unexpected effect of replacing the water molecule normally coordinated to ferric heme with a nitrogenous ligand. This phenomenon has been observed previously with certain P450 mutants (Imai and Nakamura, 1991; Matsunaga et al., 2001),and recently with highly concentrated preparations of CYP2B4 used in crystallographic studies (Scott et al., 2003). However, in none of these cases did nitrogen ligation to the heme involve the B′-C loop. Given the conformationally dynamic nature of the B′-C loop region of the P450s (Poulos, 2003), at least three possibilities can be envisioned for the structure of the iron-nitrogen ligated mutant. First, the R108H mutation might have a secondary conformational effect on basic residues that lie closer to the active site, causing their displacement toward the heme iron. However, this is considered unlikely based on the crystal structure of CYP2C9, which reveals no basic residues in the active site when (*S*)-warfarin is bound in the distal pocket (Williams et al., 2003). It is more likely that the His108 residue itself coordinates directly with the heme iron, although both intramolecular and intermolecular interactions (Scott et al., 2003) need to be considered. Studies are underway to distinguish between these two possibilities. Should the intramolecular scenario hold sway, and the B′-C loop of CYP2C9 oscillate between "out" and "in" conformations, this could have important implications for ligand recognition and delivery to the active site of CYP2C9.

In conclusion, the data presented here demonstrate different roles for Arg97, Asp293, and Arg108 in enzyme stability and substrate specificity of CYP2C9. Whereas Arg97 and Asp293 play important structural roles in the enzyme, Arg108 emerges as a critical determinant of the binding and metabolism of acidic substrates. This is based on 1) the differential selectivity of the R108F mutant for metabolism of charged and uncharged molecules and 2) loss of the type I binding spectrum for flurbiprofen and benzbromarone with this mutant.

Acknowledgments

We thank Drs. Emily Scott and Jim Halpert (University of Texas Medical Branch, Galveston) for helpful discussions on the possibility of an intermolecular interaction involving the R108H mutant.

References

Anderson BD and Conradi RA (1985) Predictive relationships in the water solubility of salts of a nonsteroidal anti-inflammatory drug. *J Pharm Sci* **74:**815–820.
Bush ED, Low LK, and Trager WF (1983) A sensitive and specific stable isotope assay for warfarin and its metabolites. *Biomed Mass Spectrom* **10:**395–398.
Busse R, Edwards G, Feletou M, Fleming I, Vanhoutte PM, and Weston AH (2002) EDHF: bringing the concepts together. *Trends Pharmacol Sci* **23:**374–380.
Chen CD, Doray B, and Kemper B (1997) Efficient assembly of functional cytochrome P450 2C2 requires a spacer sequence between the N-terminal signal anchor and catalytic domains. *J Biol Chem* **272:**22891–22897.
Dabrowski MJ, Schrag ML, Wienkers LC, and Atkins WM (2002) Pyrene-pyrene complexes at the active site of cytochrome P450 3A4: evidence for a multiple substrate binding site. *J Am Chem Soc* **124:**11866–11867.
Daikh BE, Lasker JM, Raucy JL, and Koop DR (1994) Regioselective and stereoselective epoxidation of arachidonic-acid by human cytochromes P450 2c8 and 2c9. *J Pharmacol Exp Ther* **271:**1427–1433.
Davies C, Witham K, Scott JR, Pearson A, DeVoss JJ, Graham SE, and Gillam EMJ (2004) Assessment of arginine 97 and lysine 72 as determinants of substrate specificity in cytochrome P450 2C9 (CYP2C9) *Drug Metab Dispos* **32:**431–436.
Dawson JH, Andersson LA, and Sono M (1982) Spectroscopic investigations of ferric cytochrome P-450-CAM ligand complexes. Identification of the ligand trans to cysteinate in the native enzyme. *J Biol Chem* **257:**3606–3617.
De Groot MJ, Alex AA, and Jones BC (2002) Development of a combined protein and pharmacophore model for cytochrome P450 2C9. *J Med Chem* **45:**1983–1993.
Ekins S, de Groot MJ, and Jones JP (2001) Pharmacophore and three-dimensional quantitative structure activity relationship methods for modeling cytochrome P450 active sites. *Drug Metab Dispos* **29:**936–944.
Estabrook RW and Werringloer J (1978) The measurement of difference spectra: application to the cytochromes of microsomes. *Methods Enzymol* **52:**212–220.
Falk JE (1964) *Porphyrins and Metalloporphyrins: Their General, Physical, and Coordination Chemistry and Laboratory Methods.* Elsevier, Amsterdam.
Fisslthaler B, Hinsch N, Chataigneau T, Popp R, Kiss L, Busse R, and Fleming I (2000) Nifedipine increases cytochrome P4502C expression and endothelium-derived hyperpolarizing factor-mediated responses in coronary arteries. *Hypertension* **36:**270–275.
Flanagan JU, McLaughlin LA, Paine MJI, Sutcliffe MJ, Roberts GCK, and Wolf CR (2003) Role of conserved Asp^{293} of cytochrome P4502C9 in substrate recognition and catalytic activity. *Biochem J* **370:**921–926.
Guengerich FP, Miller GP, Hanna IH, Martin MV, Leger S, Black C, Chauret N, Silva JM, Trimble LA, Yergey JA, et al. (2002) Diversity in the oxidation of substrates by cytochrome P450 2D6: lack of an obligatory role of aspartate 301-substrate electrostatic bonding. *Biochemistry* **41:**11025–11034.
Haining RL, Jones JP, Henne KR, Fisher MB, Koop DR, Trager WF, and Rettie AE (1999) Enzymatic determinants of the substrate specificity of CYP2C9: role of B′-C loop residues in providing the pi-stacking anchor site for warfarin binding. *Biochemistry* **38:**3285–3292.
Henne KR, Kunze KL, Zheng YM, Christmas P, Soberman RJ, and Rettie AE (2001) Covalent linkage of prosthetic heme to CYP4 family P450 enzymes. *Biochemistry* **40:**12925–12931.
Imai Y and Nakamura M (1991) Nitrogenous ligation at the sixth coordination position of the Thr-301 to Lys-mutated P450IIC2 heme iron. *J Biochem (Tokyo)* **110:**884–888.
Johnson EF, Wester MR, Schoch G, Yano JK, and Stout CD (2003) Structural determinants of the catalytic diversity and substrate selectivity of the CYP2C enzymes. 12th North American ISSX Meeting; Providence, RI; 2003 Oct 12–16. Abstract 16.
Jung F, Griffin KJ, Song W, Richardson TH, Yang M, and Johnson EF (1998) Identification of amino acid substitutions that confer a high affinity for sulfaphenazole binding and a high catalytic efficiency for warfarin metabolism to P450 2C19. *Biochemistry* **37:**16270–16279.
Kirton SB, Kemp CA, Tomkinson NP, St-Gallay S, and Sutcliffe MJ (2002) Impact of incorporating the 2C5 crystal structure into comparative models of cytochrome P450 2D6. *Proteins* **49:**216–231.
Lang D and Bocker R (1995) Highly sensitive and specific high-performance liquid chromatographic analysis of 7-hydroxywarfarin, a marker for human cytochrome P-4502C9 activity. *J Chromatogr Biomed Appl* **672:**305–309.
Lasker JM, Wester MR, Aramsombatdee E, and Raucy JL (1998) Characterization of CYP2C19 and CYP2C9 from human liver: respective roles in microsomal tolbutamide, S-mephenytoin and omeprazole hydroxylations. *Arch Biochem Biophys* **353:**16–28.
Locuson CW, Wahlstrom JL, Rock DA, Rock DA, and Jones JP (2003) A new class of CYP2C9 inhibitors:probing specifcity with high-affinity benzbromarone derivatives. *Drug Metab Dispos* **31:**967–971.
Martinis SA, Blanke SR, Hager LP, Sligar SG, Hoa GH, Rux JJ, and Dawson JH (1996) Probing the heme iron coordination structure of pressure-induced cytochrome P420cam. *Biochemistry* **35:**14530–14536.
Matsunaga I, Ueda A, Sumimoto T, Ichihara K, Ayata M, and Ogura H (2001) Site-directed mutagenesis of the putative distal helix of peroxygenase cytochrome P450. *Arch Biochem Biophys* **394:**45–53.
Melet A, Assrir N, Jean P, Lopez-Garcia MP, Marques-Soares C, Jaouen M, Dansette PM, Sari MA, and Mansuy D (2003) Substrate selectivity of human cytochrome P4502C9: importance of residues 476, 365, and 114 in recognition of diclofenac and sulfaphenazole and in mechanism-based inactivation by tienilic acid. *Arch Biochem Biophys* **409:**80–91.
Miners JO and Birkett DJ (1998) Cytochrome P4502C9: an enzyme of major importance in human drug metabolism. *Br J Clin Pharmacol* **45:**525–538.
Paine MJI, McLaughlin LA, Flanagan JU, Kemp CA, Sutcliffe MJ, Roberts GCK, and Wolf CR (2003) Residues glutamate 216 and aspartate 301 are key determi-

nants of substrate specificity and product regioselectivity in cytochrome P450 2D6. *J Biol Chem* **278:**4021–4027.
Payne VA, Chang YT, and Loew GH (1999) Homology modeling and substrate binding study of human CYP2C9 enzyme. *Proteins* **37:**176–190.
Poulos TL (2003) Cytochrome P450 flexibility. *Proc Natl Acad Sci* **100:**13121–13122.
Rao S, Aoyama R, Schrag M, Trager WF, Rettie A, and Jones JP (2000) A refined 3-dimensional QSAR of cytochrome P450 2C9: computational predictions of drug interactions. *J Med Chem* **43:**2789–2796.
Ridderstrom M, Masimirembwa C, Trump-Kallmeyer S, Ahlefelt M, Otter C, and Andersson TB (2000) Arginines 97 and 108 in CYP2C9 are important determinants of the catalytic function. *Biochem Biophys Res Commun* **270:**983–987.
Rodrigues AD and Lin JH (2001) Screening of drug candidates for their drug–drug interaction potential. *Curr Opin Chem Biol* **5:**396–401.
Scott EE, He AY, Wester MR, White MA, Chin CC, Halert JR, Johnson EF, and Stout CD (2003) An open conformation of mammalian cytochrome P450 2B4 at 1.6 angstrom resolution. *Proc Natl Acad Sci USA* **100:**13196–13201.
Wester MR, Johnson EF, Marques-Soares C, Dansette PM, Mansuy D, and Stout CD (2003) Structure of a substrate complex of mammalian cytochrome P4502C5 at 2.3 angstrom resolution: evidence for multiple substrate binding modes. *Biochemistry* **42:**6370–6379.
Williams PA, Cosme J, Ward A, Angove HC, Vinkovic DM, and Jhoti H (2003) Crystal structure of human cytochrome P450 2C9 with bound warfarin. *Nature (Lond)* **424:**464–468.

Address correspondence to: Dr. Allan E. Rettie, Department of Medicinal Chemistry, Box 357610, University of Washington, Seattle, WA 98195. E-mail: rettie@u.washington.edu